This manuscript was accepted for publication in Journal of Applied Polymer Science

Mechanical Behavior, Microstructure and Thermooxidation properties of Sequentially Crosslinked Ultra-High Molecular Weight Polyethylenes

R. Ríos[1], J.A. Puértolas[1,3*], V. Martínez-Nogués[1], M.J. Martínez-Morlanes[1], F.J. Pascual[1], J. Cegoñino[1,2], F.J. Medel[2,3].

[1]Instituto de Investigaciones en Ingeniería de Aragón. I3A-U. 50018 Zaragoza, Spain.

[2] Department of Mechanical Engineering. University of Zaragoza. 50018 Zaragoza. Spain.

[3]Instituto de Ciencia de Materiales de Aragón, ICMA, CSIC-Universidad de Zaragoza, 50018, Zaragoza, Spain.

*Correspondence to Prof. Francisco Javier Medel
Department of Mechanical Engineering,
Engineering and Architecture School, Universidad de Zaragoza,
E-50018, Zaragoza, Spain
Tel. : +34 976 762553
Fax. : +34 976 761957
e-mail: fjmedel@unizar.es

ABSTRACT

The aim of this study was to explore the impact of the sequential irradiation and annealing process on the microstructure, thermooxidation behaviour and mechanical properties of GUR 1050 ultra-high molecular weight polyethylene (UHMWPE) with respect to the post-irradiation annealed material. For this purpose, the effects of a variety of irradiation and annealing conditions on microstructure and mechanical properties were investigated. Differential scanning calorimetry was performed to characterize melting temperature, crystalline content and crystal thickness, whereas transmission electron microscopy provided additional insights into crystal morphology. Thermogravimetric experiments in air served to assess thermooxidation resistance and changes associated to radiation-induced crosslinking. Fatigue properties were studied from three different approaches, namely short-term cyclic stress-strain tests, long-term fatigue experiments and crack propagation behaviour. Likewise, three experimental techniques (uniaxial tensile test, impact experiments, and load to fracture of compact tension specimens) allowed evaluation of the fracture resistance. The present findings confirm sequentially crosslinked UHMWPE exhibited improved thermooxidation resistance and thermal stability compared to post-irradiation annealed UHMWPE. Also, the mechanical behaviour, including the fatigue and fracture resistance, of these materials was generally comparable regardless of the annealing strategy. Therefore, the sequential irradiation and annealing process might provide higher oxidation resistance, but not a significant improvement in mechanical properties compared to the single radiation dose and subsequent annealing procedure.

KEYWORDS: UHMWPE, Highly crosslinked polyethylenes, sequential annealing, fatigue and fracture resistance, toughness.

INTRODUCTION

Nowadays, modern highly cross-linked polyethylenes (HXLPE) have replaced conventional, gamma inert sterilized, ultra high molecular weight polyethylene (UHMWPE) for use in total hip arthroplasties[1,2]. The rationale behind the introduction of HXLPE for orthopaedic use is a dramatically improved wear resistance, which, in turn, stems from the elevated crosslink density that high gamma or electron beam radiation doses (~100 kGy) impart UHMWPE [3-5]. This beneficial property has made possible a significant reduction in the incidence of revisions that historical, gamma air sterilized, and conventional UHMWPE inserts experienced due to osteolytic reactions and eventual aseptic loosening triggered by UHMWPE wear debris particulate[6]. Despite its positive effect on wear resistance, irradiation unavoidably generates free radicals, which have the potential to initiate the oxidation cycle of HXLPE. To prevent long-term degradation in the presence of oxygen, post-irradiation thermal treatments have been necessary to eliminate, or at least reduce, radiation-induced free radicals[7]. In general, thermal treatments used in first generation HXLPE production can be classified as annealing or remelting depending on whether or not they were conducted below the melting temperature. Despite the excellent wear resistance of current HXLPE, they present some drawbacks. On one hand, annealed HXLPE contain residual free radicals, and therefore *in vivo* oxidation may result in material embrittlement, ultimately compromising the mechanical performance of the insert. High radiation doses followed by remelting, on the other hand, considerably reduce the fatigue and fracture properties of UHMWPE [8-12]. Although the clinical performance of HXLPE in total hip arthroplasty has been satisfactory for the first decade of use [6], there is growing evidence of high oxidation in non-load bearing regions of retrieved annealed hip inserts [13], and early crack initiation in few, case studies, remelted retrievals [14,15]. With regard to total knee arthroplasty, annealed and remelted HXLPE are not generally recommended, since in vivo oxidation, and rapid cracking, respectively, might have dramatic consequences under the more demanding conditions of the knee joint[16].

Second-generation highly crosslinked polyethylenes represent an attempt to simultaneously provide oxidative stability and preserved mechanical properties. Three main strategies have been proposed, namely sequential irradiation and annealing, incorporation of antioxidants (i.e. vitamin E) by blending or diffusion, and mechanical annealing. Vitamin E acts as a scavenger of radiation-induced free radicals in UHMWPE [17-19], whereas solid-state deformation below the melting point of highly crosslinked polyethylenes provides enhanced strength and good oxidative stability [20]. The basis for sequentially irradiated and annealed UHMWPE is that the annealing treatment would be more effective eliminating free radicals produced by 30 kGy-irradiation steps, since chain mobility is higher when crosslink density is low. Thus, three consecutive irradiation and annealing cycles would provide the excellent wear resistance associated to high radiation doses (~100 kGy) as well as oxidative stability, without negatively affecting crystallinity and mechanical properties [21-23]. Terminal gas plasma sterilization completes the production of commercial sequentially irradiated and annealed UHMWPE. However, some contradictory results appear in the literature concerning the improvement in mechanical properties obtained with this new sequential irradiation and annealing process [23-25].

In the context presented above, the current work aims at comparing several second generation, sequentially irradiated and annealed UHMWPEs with first generation, post-irradiation annealed, HXLPE from mechanical and thermooxidation perspectives. The correlation between microestructural features and mechanical properties was also studied.

MATERIALS AND METHODS

Materials

We used GUR 1050 UHMWPE in the form of compression-molded sheets (Orthoplastic Medical Ltd.; Lancashire, UK) as raw material. Crosslinking was achieved by three consecutive 30 kGy gamma irradiation in air steps (Aragogamma S.A.; Barcelona, Spain). Post-irradiation annealed UHMWPE was obtained performing a terminal annealing treatment at 130º C for 8 hours in a vacuum oven (Weiss-Gallenkamp; Loughborough, UK). Sequentially irradiated and annealed UHMWPEs were produced conducting identical annealing treatments after all or some of the 30 kGy irradiation steps. A final machining step was necessary to remove the outer, oxidized, layer (~2-3 mm) of the irradiated and annealed pre-forms, thus obtaining mechanical specimens ready to test. Typically, we used unirradiated UHMWPE as control material, but in some cases also single-dose (90 kGy) irradiated and three-step irradiated (30-30-30) UHMWPEs without further annealing, to discriminate the separate effects of irradiation and annealing. Thus, the seven material groups studied will be referred to as virgin or unirradiated, G0 (30-30-30), G1 (30-30-30A), G2 (30-30A-30A), G3 (30A-30A-30A), G4 (30A-30-30), and G5 (90), where G, 30, and A stand for gamma irradiated, a single 30 kGy irradiation step, and annealing, respectively. It is worth noting that G1, and G3 were obtained following procedures similar to those used to produce commercially available post-irradiation annealed HXLPE, and the second generation, sequentially crosslinked, HXLPE, respectively.

Differential Scanning Calorimetry and Thermogravimetry

Differential Scanning Calorimetry (DSC) experiments were conducted in air using a Dynamic Scanning Calorimeter (TA Instruments Q20). At least three samples ($n \geq 3$) per material group were heated from room temperature to 200 ºC at a 10 ºC/min rate. The area below the first-heating DSC curves from 80ºC to 160ºC, normalized by 290 J/g as the enthalpy of melting of a 100 % crystalline polyethylene, served to calculate crystallinity contents. The melting transition temperature was registered as the peak temperature of the melting endotherm.

Thermogravimetric (TG) experiments were carried out in air using a TA Instrument Q5000 thermobalance (accuracy: 10^{-4} mg). 6 mg-samples (n≥3 per material group) were heated from room temperature to 800 ºC at a 10 ºC/min rate. The main features in decomposition curves were documented and analyzed following recently reported guidelines [26].

Transmission Electron Microscopy analysis

Transmission Electron Microscopy (TEM) was performed to observe the microstructure of all the materials using a Jeol 100CX microscope operating at 100 kV. Appropriate specimen preparation involving clorosulphonic staining of thin films was necessary to make the samples ready for TEM, as reported elsewhere[27]. 20,000x and 60,000x magnification micrographs were taken and analysed using Digital Micrograph 3.3.1 (Gatan Inc., Pleasanton, CA, USA) to measure changes in lamellar thickness after irradiation and annealing stabilization.

Uniaxial tensile tests

Uniaxial tensile tests ($n \geq 3$) per ASTM D638 were performed in an electromechanic Instron machine on type M-I specimens, at T = 23 ± 2 ºC, with a displacement rate of 5 mm/min (initial nominal strain rate ~0.002 s^{-1}). In addition to typical parameters, such as yield stress, elastic modulus, and ultimate stress and strain, work to fracture values were calculated from engineering stress-strain plots.

Cyclic Stress-Strain, Long-Term Fatigue and Fatigue Crack Propagation Experiments

The fatigue behavior was characterized by means of three experimental techniques. First, cyclic stress–strain experiments were conducted on tensile specimens for up to 50 cycles. A displacement rate of 15 mm/min (initial nominal strain rate 0.005 s^{-1}), and a maximum nominal stress, σ_{max}, of 16 MPa (stress ratio R ~ 0) were chosen to conduct these experiments. At least three samples ($n \geq 3$) per material group were tested in an Instron 5565 machine at 24 ± 1 °C. These short-term cyclic experiments provided information about the total plastic strain reached, $\varepsilon(50)$, and the secant modulus at the first cycle, $E_s(1c)$, which are measures of the material softening, and stiffness, respectively.

Second, long-term fatigue tests, S/N stress-life experiments, were performed on dog bone specimens using a servohydraulic Instron 8032 machine and following ASTM E606 guidelines. These tests ran under load control following a sine waveform (frequency 1 Hz; stress ratio R~0). The strain was continuously monitored employing an extensometer and the testing temperature was 23 ± 2 ºC. The selected failure criterion was the number of cycles needed to reach a 12 % strain level, as in previous studies[9]. This strain level is close to strain maxima (12-15%) registered in UHMWPE tibial components, and has been connected to the appearance of fatigue-induced microscopic defects[9,28,29].

Third, near-threshold fatigue crack propagation (FCP) experiments were performed on standard compact tension specimens per ASTM E647. All compact specimens were pre-cracked using a razor blade. A digital camera allowed crack growth monitoring and gradual crack length assessments. At least three specimens ($n \geq 3$) were tested per material group and they underwent tension cycling (frequency 5 Hz) with R = 0.1. $\Delta K_{inception}$ values and Paris coefficients were obtained from crack propagation curves.

Toughness Characterization

Impact Izod tests (n ≥ 3 per material group) were carried out at 23 ± 2 ºC on double-notched specimens following ASTM F648 guidelines. On the other hand, work to fracture values obtained as the area below the engineering stress-strain curves of tensile experiments gave an estimation of toughness in a quasi-static situation. Finally, compact tension specimens with dimensions complying ASTM D6068-02 (width 20 mm, thickness 10 mm and original crack length 10 mm) were loaded to fracture in an attempt to additionally characterize the toughness behaviour. Load-displacement curves were registered and analyzed to obtain relevant data.

Statistical analysis

Student´s t-tests served to detect significant differences between the thermal, thermogravimetric and mechanical properties of the studied material groups. A level of $p < 0.05$ was selected as indicative of significance.

RESULTS and DISCUSSION

Differential Scanning Calorimetry and Thermogravimetry

Both post-irradiation annealing and sequential irradiation-annealing caused important changes in the microstructure of UHMWPE. Thus, DSC curves revealed irradiation was responsible for significant 6 °C and 12% raises in melting temperature and crystallinity, respectively, as compared with virgin UHMWPE (Table 1). Both post-irradiation and sequential annealing treatments did not affect melting temperature of as-irradiated UHMWPE, but took crystalline contents back to the level (52-54%) of the unirradiated polymer. Also, materials subjected to two or more irradiation-annealing cycles, G2 and G3, developed an additional endothermic peak at about the annealing temperature (~126 ºC; Figure 1). In contrast, post-irradiation annealed UHMWPE, G1, only exhibited a small shoulder at the same temperature. Finally, no significant differences ($p > 0.05$) were detected between the melting temperature and crystallinity of both as-irradiated UHMWPE materials, G0 and G5. The present findings appear to be consistent with the occurrence of radiation-induced recrystallization as proposed by Premnath and colleagues[30], on one hand, and partial melting, lamellar thickening and crystallization of smaller crystals during annealing[31,32]. Together, these phenomena would explain the elevated melting temperature, and the appearance of an additional, smaller, endothermic peak in the case of sequentially crosslinked materials. First, molecular rearrangements triggered by irradiation allowed secondary recrystallization onto the surface of original lamellae resulting in elevated melting temperature and crystallinity. This radiation-induced crystallinity increase was lost upon 8 hours annealing at 130 °C, suggesting that partial melting of lamellar crystals prevailed over lamellar thicknening and crystallization of small crystals. The sequential annealing strategy, however, did not imply an accumulative decrease in crystallinity, probably due to comparatively higher chain mobility (i.e. lower crosslink density), which would favor lamellar thickening during the annealing steps.

The thermooxidation behavior of UHMWPE was also clearly affected by crosslinking and annealing processes. All thermogravimetric decomposition curves showed a very small but detectable mass increase associated with thermooxidation of the polymer followed by an abrupt weight loss due to thermal degradation (Figure 2A-B). The onset of the thermooxidation process, denoted T_B, reflects the susceptibility to oxidation, as reported previously [26]. In this study, both as-irradiated polyethylenes, G0 and G5, exhibited the lowest T_B values ($p<0.05$), and a significant decrease in T_B was also observed for post-irradiation annealed UHMWPE, G1, and for crosslinked materials subjected to one or two sequential irradiation-annealing steps, G2 and G4 ($T_B \sim 141$-144 °C; $p \leq 0.003$; Table 1). Overall, these data suggest that the former annealing treatments did not succeed in quenching radiation-induced free radicals and, therefore, in providing complete oxidative stability. This was probably because they were not able to eliminate free radicals trapped in crystalline regions, yielding materials with high susceptibility to oxidation. Three irradiation-annealing steps, however, did not result in a T_B decrease, but in a significant shift towards higher temperatures as registered for G3 specimens ($T_B \sim 167$ °C; $p < 0.0001$; Figure 3B). Although thermooxidation could not be completely avoided in sequentially crosslinked materials, the significantly delayed weight gain might be indicative of comparatively higher oxidation resistance. In regard to results corresponding to temperatures at maximum weight, T_0, they followed a trend similar to that of T_B data (Table 1).

The beginning of the thermal degradation, indicated by T_1 (Figure 2A), was also significantly affected by crosslinking and stabilization processes. They provoked a gradual increase from about 375 ºC to almost 400 ºC for unirradiated UHMWPE and sequentially crosslinked UHMWPEs, G3, respectively ($p < 0.0002$). Irradiation processes without further annealing steps also resulted in increased thermal stability ($T_1 \sim 390$ ºC), which was slightly higher in the case of the single-step irradiated UHMWPE (G5). The present thermogravimetric results are coherent with crosslink density data trends reported in the literature[5,9]. Previous studies have reported that sequentially annealed UHMWPE exhibits higher crosslink density than post-irradiation annealed UHMWPE[23]. Crosslinks between polymeric chains are, in turn, responsible for a concomitant molecular weight increase, and thermal degradation typically begins at increasingly higher temperatures as the molecular weight of the polymer grows [33]. In this sense, researchers have confirmed higher thermal stability, that is higher T_I, of irradiated polyethylenes [34]. Although admittedly the lack of crosslink density assessments in this study impedes to draw definite conclusions, there appears to be a connection between elevated crosslinked density and enhanced thermal stability in orthopaedic UHMWPEs.

Transmission Electron Microscopy analysis

TEM micrographs of unirradiated UHMWPE showed the typical features of a semicrystalline polymer with randomly oriented crystal lamellae immersed in the amorphous region, which appeared as a dark grey region (Figures 3A-E). The average lamellar thickness of virgin UHMWPE was 29±3 nm, and upon irradiation crystal thickness experienced a small, but statistically significant, increase up to 32±3 nm ($p < 0.0001$). In contrast, the combination of crosslinking and stabilization processes generally resulted in a significant decrease of this property. Sequentially crosslinked, G3, materials were the only exception as they presented crystal thicknesses similar (30±3 nm; $p>0.42$) to that of unirradiated specimens. The more restricted chain mobility in post-irradiation annealed, G1, and G2 UHMWPEs could inhibit crystal thickening during annealing, yielding thinner lamellae (27±2, and 26±3 nm, respectively; $p<0.0001$ with respect to unirradiated, G0 and G3 UHMWPEs). Lamellar thickening mechanisms, in contrast, would be favored during annealing in sequentially crosslinked materials, G3, due to higher chain mobility.

Uniaxial tensile results

Irradiation and stabilization treatments caused considerable changes in mechanical parameters. Both post-irradiation annealed and sequentially crosslinked UHMWPEs experienced a strong decrease (~50%) in ductility as reflected by strain to fracture results ($p<0.0001$; Table 2 and Figure 4). The fracture stress also decreased after crosslinking and stabilization ($p\leq0.02$ with respect to unirradiated UHMWPE), but this parameter was almost identical for the three sequentially crosslinked UHMWPEs, G1, G2 and G3 ($p>0.54$). As-irradiated materials, G0 and G5, exhibited slightly higher yield stresses, fracture stresses, and ultimate strains than sequentially crosslinked materials.

Cyclic Stress-Strain, Long-Term Fatigue and Crack Propagation Behavior

Cyclic stress-strain experiments confirmed a significant decrease in material softening, $\varepsilon(50)$, upon irradiation (8.3 ± 0.9 and 4.3 ± 0.2 for virgin and as-irradiated, G0, UHMWPEs, respectively; $p<0.0001$). However, this positive decrease was lost when irradiation and annealing processes were combined. Thus, material softening went down to 7.6 ± 0.8, 9.0 ± 1.4 and 8.5 ± 1.6 for post-irradiation, G1, and sequentially annealed, G2 and G3, materials, respectively ($p\leq0.0008$ with respect to G0 UHMWPE). Likewise, irradiation turned UHMWPE into a stiffer material based on secant modulus results, but, again, the combination of irradiation and annealing processes reverted this change even below the levels of uncrosslinked UHMWPE (Table 2).

The combined effects of irradiation and annealing processes caused substantial deterioration of the fatigue strength of unirradiated UHMWPE, regardless of the annealing strategy as shown in the present stress-life, S-N, ($S = A \log(N) + B$; A, and B fitting parameters) experiments (Figure 5). In particular, the introduction of annealing treatments between the second and third irradiation steps (i.e., G2 material) did not imply an improvement in long-term fatigue properties, but further reduction in fatigue strength compared to G1 and unirradiated UHMWPEs. Furthermore, each annealing step appeared to decrease the slope of the S-N curve (Figure 5). Most likely, annealing treatments were responsible for the main decrease in fatigue resistance, since irradiation without further annealing has been demonstrated to slightly augment the fatigue strength of e-beam irradiated UHMWPEs[9]. Despite the registered drop in fatigue resistance upon annealing, sequentially crosslinked UHMWPE, G3, appeared to have long-term fatigue performance closer to that displayed by unirradiated UHMWPE specimens. As proposed elsewhere, there seems to be a direct relation between mechanical behavior and microstructure for highly crosslinked UHMWPEs [8,9,35]. Thus, irradiation results in crystal thickening, which, in turn, is responsible for an improvement of the fatigue life in long-term experiments. Also, a two hours annealing has been reported to imply a decrease in lamellar thickness compared to as-irradiated UHMWPE, and, coherently, to demonstrate a reduced fatigue strength [9]. The negative impact on fatigue behavior of longer annealing steps (8 hours) found in this study appear to be compensated to some extent introducing the sequential irradiation-annealing strategy.

The microstructural changes induced by irradiation caused substantial reductions in crack propagation resistance behavior, regardless of the stabilization strategy. Fatigue crack propagation results showed two different regions in the log-log plots of crack growth rate, (da/dN), versus stress intensity factor range (ΔK) (Figure 6). The first region matched the slow crack growth regime, whereas the second one represented the intermediate crack growth or Paris equation regime ($da/dN = C\ (\Delta K)^m$; C and m are constants). A fatigue crack inception stress intensity range ($\Delta k_{inception}$) could be defined as the intersection of the first regime, nearly vertical, curve with the x-axis, at a value of $da/dN = 10^{-6}$ m/cycle. This approach gave the stress intensity threshold that must be overcome to initiate the propagation of a static crack and permitted comparison between materials. The second region fitted to a linear trend, which its slope, m, provided information about how fast the crack propagate once it started to grow. Fast-fracture regime was reached at the end of all the experiments. The unirradiated material presented the highest Δk at crack inception (2.2±0.1 MPa m$^{1/2}$), whereas the corresponding Δk of the crosslinked UHMWPEs (G1, G2 and G3) dropped to values close to 1.6 MPa m$^{1/2}$ (Table 3). This finding was not unexpected, as previous studies have confirmed remarkably drops in stress intensity factor at crack inception, $\Delta k_{inception}$, after irradiation [8-11,35]. Thus, the greater the radiation dose, the higher crosslink density and the lower the $\Delta k_{inception}$. The elevated crosslink density imparted by irradiation reduces the deformation modes of the amorphous region, and therefore cracks grow more easily in crosslinked UHMWPEs [36]. On the other hand, no significant differences ($p > 0.05$) were found regarding the crack inception behavior among crosslinked UHMWPEs. It can be concluded that the annealing strategy, terminal or sequential, scarcely affected the crack propagation resistance, confirming crack inception is mainly governed by crosslink density in crosslinked UHMWPEs. Finally, sequentially crosslinked materials, G2 and G3, had less steep slopes (lower m coefficients) than unirradiated and post-irradiation annealed UHMWPEs (Table 3). This fact might indicate that lower stress levels are needed to reach similar crack growth rates.

Toughness behavior

The radiation dose absorbed was the key parameter governing the fracture resistance of the various UHMWPE formulations. A significant decrease in impact toughness was confirmed for crosslinked UHMWPEs compared to the unirradiated polymer ($p<0.0001$). Thus, impact toughness dropped about a 40 % upon irradiation and a 50 % after crosslinking and stabilization processes (Table 4). As mentioned before, the elevated crosslink density limits the ductility, and also its fracture resistance, as the crosslinked network prevents the polymer from reaching high deformations[35].

Crystallinity drops registered after performance of annealing treatments also negatively affected the fracture resistance of crosslinked UHMWPEs, although to a much lesser extent. However, the introduction of more than one annealing step had no further influence on impact toughness, as no significant differences could be detected among crosslinked and stabilized UHMWPEs regardless of the annealing strategy. Work to fracture results followed a trend similar to that of impact results. Unirradiated UHMWPE had the highest work to fracture ($p<0.0001$), whereas crosslinked UHMWPE exhibited very low values, mostly due to the loss in ductility. The energy needed to fracture crosslinked materials decreased a little bit further as more annealing steps were introduced (Table 4). Finally, load displacement curves to fracture corresponding to compact tension specimens revealed a similar behaviour, with unirradiated UHMWPE needing high loads and displacements to reach fracture, while crosslinked UHMWPEs had much lower values (Figure 7). Again, no significant differences were found among crosslinked UHMWPEs.

Commercially available sequentially crosslinked UHMWPE is claimed to have excellent oxidation resistance (no detectable free radicals) and superior mechanical properties compared to its post-irradiation annealed predecessor [23,24,37]. It is worth mentioning that the UHMWPE resins used to produce these formulations are different. The manufacturer replaced the GUR 1050 UHMWPE resin employed to fabricate post-irradiation annealed UHMWPE with GUR 1020 resin to produce the sequentially annealed formulation. The latter resin is a lower molecular weight powder, and UHMWPE materials produced from this resin have been reported to exhibit improved mechanical properties than those manufactured from GUR 1050[38]. So, it is unclear whether the improvement stems from the annealing strategy or the UHMWPE resin. Our study suggests that oxidation resistance seems to be superior for sequentially annealed

UHMWPEs from a thermooxidation perspective. However, the mechanical improvement obtained after introduction of three sequential irradiation-annealing steps appears to be quite limited, at least when GUR 1050 resin is used as base material.

Obviously, the present study is not free of some limitations. First, thermooxidation parameters might not necessarily correlate with oxidation indices measured after shelf-aging or *in vivo* oxidation conditions. The orthopaedic community generally relies on standard accelerated aging protocols to explore the oxidative stability of alternative polyethylenes and to categorize them. However, accelerated aging protocols have not always provided an exact correspondence to oxidation indices and regional distribution of oxidation maxima found in shelf aged implants or retrievals. Remelted polyethylenes represent an interesting example as these materials performed very well after accelerated aging[39], but recent evidence suggests no complete oxidation resistance was achieved[40]. We chose to perform thermogravimetry since it provides a faster first screening regarding oxidative stability of the molten polymer. Second, cyclic stress-strain and long-term fatigue experiments are not intended to confirm the suitability of the studied polyethylene materials as acetabular liners or tibial inserts, or to predict an optimal clinical performance. These mechanical tests do not take into account complex load patterns (biaxial or triaxial stress states), and, on the other hand, the clinical performance of the artificial joint depends on a variety of patient, surgical, design and material factors.

CONCLUSIONS

This study provides evidence that the introduction of sequential irradiation-annealing processes may improve the resistance to oxidation as compared to post-irradiation annealed UHMWPEs. The microstructural characterization of sequentially crosslinked UHMWPEs also confirmed crystal thickness and crystallinity contents similar to those of the unirradiated polymer, whereas the thermogravimetric behavior suggested this material had the highest crosslink density. The anticipated improvement in mechanical properties, however, appears to be more limited, as the mechanical, crack propagation and fracture resistance properties were generally comparable to those of post-irradiation annealed and G2 (two sequential irradiation and annealing steps) UHMWPEs.

ACKNOWLEDGEMENTS

Research funded by the Comisión Interministerial de Ciencia y Tecnología (CICYT), Spain. Project: MAT 2006-12603-C02-01.

REFERENCES

1. Kurtz, S.; Medel, F. J.; Manley, M., Current Orthopaedics 22, 392 2008.
2. Medel, F. J.; Kurtz, S. M.; Hozack, W. J.; Parvizi, J.; Purtill, J. J.; Sharkey, P. F.; MacDonald, D.; Kraay, M. J.; Goldberg, V.; Rimnac, C. M., J Bone Joint Surg Am 91, 839 2009.
3. McKellop, H.; Shen, F. W.; Lu, B.; Campbell, P.; Salovey, R., J Orthop Res 17, 157 1999.
4. Kurtz, S. M.; Muratoglu, O. K.; Evans, M.; Edidin, A. A., Biomaterials 20, 1659 1999.
5. Muratoglu, O. K.; Bragdon, C. R.; O'Connor, D. O.; Jasty, M.; Harris, W. H.; Gul, R.; McGarry, F., Biomaterials 20, 1463 1999.
6. Kurtz, S. M.; Medel, F. J.; MacDonald, D. W.; Parvizi, J.; Kraay, M. J.; Rimnac, C. M., J Arthroplasty 25, 67 2010.
7. Kurtz, S. M., The UHMWPE Biomaterials Handbook: Ultra-High Molecular Weight Polyethylene in Total Joint Replacement and Medical Devices (2nd Edition); Academic Press: Burlington, MA, 2009.
8. Baker, D. A.; Bellare, A.; Pruitt, L., J Biomed Mater Res A 66, 146 2003.
9. Medel, F. J.; Pena, P.; Cegonino, J.; Gomez-Barrena, E.; Puertolas, J. A., J Biomed Mater Res B Appl Biomater 83, 380 2007.
10. Oral, E.; Malhi, A. S.; Muratoglu, O. K., Biomaterials 27, 917 2006.
11. Gencur, S. J.; Rimnac, C. M.; Kurtz, S. M., Biomaterials 27, 1550 2006.
12. Puertolas, J. A.; Medel, F. J.; Cegonino, J.; Gomez-Barrena, E.; Rios, R., J Biomed Mater Res B Appl Biomater 76, 346 2006.
13. Kurtz, S. M.; Austin, M. S.; Azzam, K.; Sharkey, P. F.; MacDonald, D. W.; Medel, F. J.; Hozack, W. J., J Arthroplasty 25, 614 2010.
14. Furmanski, J.; Kraay, M. J.; Rimnac, C. M., J Arthroplasty2010.
15. Furmanski, J.; Anderson, M.; Bal, S.; Greenwald, A. S.; Halley, D.; Penenberg, B.; Ries, M.; Pruitt, L., Biomaterials 30, 5572 2009.
16. Ries, M. D., J Arthroplasty 20, 59 2005.
17. Oral, E.; Christensen, S. D.; Malhi, A. S.; Wannomae, K. K.; Muratoglu, O. K., J Arthroplasty 21, 580 2006.
18. Oral, E.; Greenbaum, E. S.; Malhi, A. S.; Harris, W. H.; Muratoglu, O. K., Biomaterials 26, 6657 2005.
19. Oral, E.; Rowell, S. L.; Muratoglu, O. K., Biomaterials 27, 5580 2006.
20. Kurtz, S. M.; Mazzucco, D.; Rimnac, C. M.; Schroeder, D., Biomaterials 27, 24 2006.
21. Wang, A.; Yau, S. S.; Essner, A.; Herrera, L.; Manley, M.; Dumbleton, J., J Arthroplasty 23, 559 2008.
22. Dumbleton, J. H.; D'Antonio, J. A.; Manley, M. T.; Capello, W. N.; Wang, A., Clin Orthop Relat Res 453, 265 2006.
23. Wang, A.; Zeng, H.; Yau, S. S.; Essner, A.; Manely, M.; Dumbleton, J., Journal of Physics D-Applied Physics 39, 3213 2006.
24. Dumbleton, J. H.; D'Antonio, J. A.; Manley, M. T.; Capello, W. N.; Wang, A., Clinical Orthopaedics and Related Research, 265 2006.
25. Morrison, M. L.; Jani, S., Journal of Biomedical Materials Research Part B-Applied Biomaterials 90B, 87 2009.
26. Martinez-Morlanes, M. J.; Medel, F. J.; Mariscal, M. D.; Puertolas, J. A., Polymer Testing 29, 425 2010.

27. Medel, F. J.; Garcia-Alvarez, F.; Gomez-Barrena, E.; Puertolas, J. A., Polymer Degradation and Stability 88, 435 2005.
28. Baker, D. A.; Pruitt, L.; Bellare, A., Journal of Materials Science Letters 20, 1163 2001.
29. Urries, I.; Medel, F. J.; Rios, R.; Gomez-Barrena, E.; Puertolas, J. A., J Biomed Mater Res B Appl Biomater 70, 152 2004.
30. Premnath, V.; Bellare, A.; Merrill, E. W.; Jasty, M.; Harris, W. H., Polymer 40, 2215 1999.
31. Fischer, E. W., Pure Applied Chemistry 31, 19 1972.
32. Matsuda, H.; Aoike, T.; Uehara, H.; Yamanobe, T.; Komoto, T., Polymer 42, 5013 2001.
33. Poutsma, M. L., Macromolecules 36, 8931 2003.
34. Krupa, I.; Luyt, A. S., Polymer Degradation and Stability 71, 361 2001.
35. Medel, F. J.; Furmanski, J. In UHMWPE Biomaterials Handbook (Second Edition); Steven, M. K.; Ph.D.A2 - Steven M. Kurtz, P. D., Eds.; Academic Press: Boston, 2009.
36. Lin, L.; Argon, A. S., Journal of Materials Science 29, 294 1994.
37. Wang, A. G.; Yau, S. S.; Essner, A.; Herrera, L.; Manley, M.; Dumbleton, J., Journal of Arthroplasty 23, 559 2008.
38. Currier, B. H.; Currier, J. H.; Collier, J. P.; Mayor, M. B., J Biomed Mater Res 53, 143 2000.
39. Muratoglu, O. K.; Merrill, E. W.; Bragdon, C. R.; O'Connor, D.; Hoeffel, D.; Burroughs, B.; Jasty, M.; Harris, W. H., Clin Orthop Relat Res, 253 2003.
40. Currier, B. H.; Van Citters, D. W.; Currier, J. H.; Collier, J. P., J Bone Joint Surg Am 92, 2409 2010.

Table 1. Thermal and thermogravimetric parameters (mean ± standard deviation) obtained from DSC and TG experiments for unirradiated, post-irradiation annealed, and sequentially crosslinked UHMWPEs.

	DSC			TG		
Material	Shoulder Temperature (ºC)	Melting Temperature (ºC)	Crystallinity (%)	T_B (ºC)	T_0 (ºC)	T_1 (ºC)
Unirradiated	N/A	136.2 ± 0.3^{a}	51.9 ± 0.7^{a}	151.9 ± 0.6^{a}	214.9 ± 0.6^{a}	374.4 ± 3.8^{a}
G0 (30-30-30)	N/A	142.1 ± 1.1^{b}	58.7 ± 0.5^{b}	140.7 ± 0.1^{b}	219.3 ± 0.4	388.0 ± 2.4^{b,c}
G1 (30-30-30A)	125.5 ± 1.6	141.0 ± 0.6^{b}	53.1 ± 1.0^{c}	142.8 ± 3.4^{b}	212.6 ± 0.9^{b}	384.3 ± 4.7^{b}
G2 (30-30A-30A)	126.0 ± 0.2	141.1± 0.6^{b}	51.6 ± 1.1^{c}	144.4 ± 1.1^{b}	211.8 ± 1.7^{b}	390.7 ± 3.6^{b}
G3 (30A-30A-30A)	127.5 ± 0.3	141.4 ± 0.5^{b}	53.7 ± 2.1^{c}	167.6 ± 2.5^{c}	233.0 ± 0.8^{c}	397.6 ± 5.0^{b,d}
G4 (30A-30-30)	N/A	143.2 ± 0.9^{b}	58.8 ± 0.6^{b}	141.2 ± 0.8^{b}	216.2 ± 1.9	391.5 ± 1.2^{b}
G5 (90)	N/A	141.1 ± 0.5^{b}	58.8 ± 0.2^{b}	139.9 ± 0.4^{b}	217.8 ± 3.5	396.1 ± 12.2^{b}
		$p < 0.0001^{a,b}$	$p < 0.0001^{a,b}$ $p < 0.0001^{b,c}$	$p \leq 0.003^{a,b}$; $p < 0.0001^{a,c;\ b,c}$	$p \leq 0.03^{a,b}$; $p < 0.0001^{a,c;\ b,c}$	$p \leq 0.023^{a,b}$ $p < 0.0054^{c,d}$

N/A: Not applicable

Table 2. Mechanical parameters (mean ± SD) obtained from uniaxial tension and cyclic stress-strain experiments for unirradiated, post-irradiation annealed and sequentially crosslinked UHMWPE materials.

	Uniaxial Tension			50 Cycles Stress-Strain Testing	
Material	Yield stress (MPa)	Fracture Stress (MPa)	Fracture Strain	$E_S(1c)$ (MPa)	$\varepsilon_{16MPa}(50c)$
Unirradiated	19.0 ± 0.2	36.3 ± 1.8^{a}	8.7 ± 0.5^{a}	380 ± 28^{a}	8.3 ± 0.9^{a}
G0 (30-30-30)	20.8 ± 0.1^{a}	36.7 ± 0.3	4.7 ± 0.1^{b}	494 ± 13^{b}	4.3 ± 0.2^{b}
G1 (30-30-30A)	17.7 ± 0.3^{b}	30.4 ± 1.8^{b}	4.3 ± 0.2^{b}	372 ± 16^{a}	7.6 ± 0.8^{c}
G2 (30-30A-30A)	19.4 ± 0.2^{b}	31.6 ± 3.4^{b}	4.3 ± 0.6^{b}	358 ± 13^{a}	9.0 ± 1.4^{c}
G3 (30A-30A-30A)	17.9 ± 1.2^{b}	31.1 ± 2.3^{b}	4.5 ± 0.2^{b}	367 ± 22^{a}	8.5 ± 1.6^{c}
G4 (30A-30-30)	20.2 ± 0.1	35.6 ± 2.1	4.8 ± 0.3^{b}	489 ± 11^{b}	4.4 ± 0.1^{b}
G5 (90)	20.1 ± 0.3	32.4 ± 2.6	4.6 ± 0.4^{b}	483 ± 15^{b}	4.8 ± 0.1^{b}
	$p \leq 0.005^{a,b}$	$p \leq 0.02^{a,b}$ $p > 0.54^{b}$	$p < 0.0001^{a,b}$	$p < 0.0001^{a,b}$	$p \leq 0.0002^{a,b}$ $p \leq 0.0008^{b,c}$

Table 3. Stress-intensity levels at crack inception (mean ± SD) for virgin, post-irradiation annealed and sequentially annealed UHMWPEs.

Material	$\Delta K_{inception}$ (MPam$^{1/2}$)	m
Unirradiated	2.22 ± 0.06	12.1 ± 2.0
G1 (30-30-30A)	1.49 ± 0.03	12.9 ± 0.8
G2 (30-30A-30A)	1.58 ± 0.08	8.6 ± 0.3
G3 (30A-30A-30A)	1.51 ± 0.03	7.1 ± 1.5
B100A*	1.49 ± 0.06	12.9 ± 0.8

*Data reported in reference [9] corresponding to 100 kGy e-beam irradiated and annealed UHMWPE

Table 4. Estimations of toughness behavior (mean ± SD) from uniaxial tension and impact tests.

Material	Work to Fracture (MPa or MJ/m3)	Impact Toughness (kJ/m2)
Unirradiated	209.7 ± 20.7^{a}	100.9 ± 10.3^{a}
G0 (30-30-30)	116.5 ± 4^{b}	62.6 ± 4.7^{b}
G1 (30-30-30A)	88.8 ± 6.4^{b}	$47.1 \pm 2.9^{b,c}$
G2 (30-30A-30A)	93.3 ± 19.4^{b}	$47.8 \pm 2.6^{b,c}$
G3 (30A-30A-30A)	94.1 ± 7.1^{b}	$47.9 \pm 5.2^{b,c}$
G4 (30A-30-30)	114.8 ± 10.7^{b}	N/A
G5 (90)	105.3 ± 12.8^{b}	N/A
	$p < 0.0001^{a,b}$	$p < 0.0001^{a,b}$ $p \leq 0.0015^{b,c}$

N/A: Not available

FIGURE CAPTIONS

Figure 1. First-heating DSC curves corresponding to virgin, post-irradiation annealed (303030A or G1), and sequentially crosslinked (3030A30A or G2, and 30A30A30A or G3) UHMWPEs.

Figures 2A-B. Thermogravimetric decomposition curves corresponding to virgin, post-irradiation annealed, and sequentially crosslinked UHMWPEs, (A). A close-up view within the 125 – 275 °C range revealed a mass increase associated to thermooxidation of the polymers, (B).

Figures 3A-E. TEM micrographs (x60,000) of virgin, (A), as-irradiated (B), post-irradiation annealed, (C), sequentially crosslinked G2, (D), and sequentially crosslinked G3, (E), UHMWPEs.

Figure 4. Typical engineering stress-strain curves obtained from uniaxial tensile tests for virgin, post-irradiation annealed, and sequentially crosslinked UHMWPEs.

Figure 5. Stress–life curves for virgin, post-irradiation annealed, and sequentially crosslinked UHMWPEs.

Figure 6. Fatigue crack propagation curves corresponding to virgin, post-irradiation annealed, and sequentially crosslinked UHMWPEs.

Figure 7. Load-displacement curves to fracture corresponding to compact tension specimens of virgin, post-irradiation annealed, and sequentially crosslinked, G3, UHMWPEs.

FIGURE 1

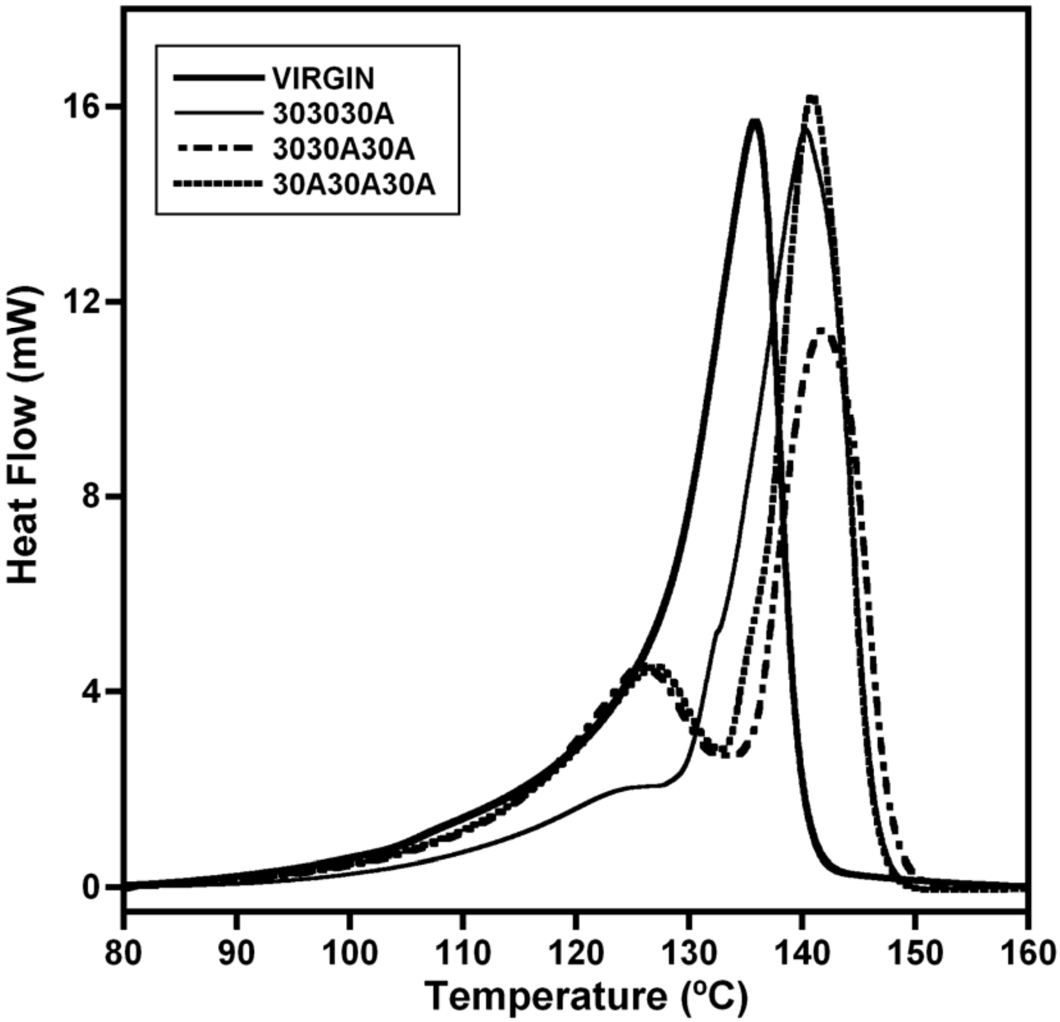
VIRGIN
303030A
3030A30A
30A30A30A
Heat Flow (mW)
0
4
8
12
16
80
90
100
110
120
130
140
150
160
Temperature (ºC)

FIGURES 2A-B

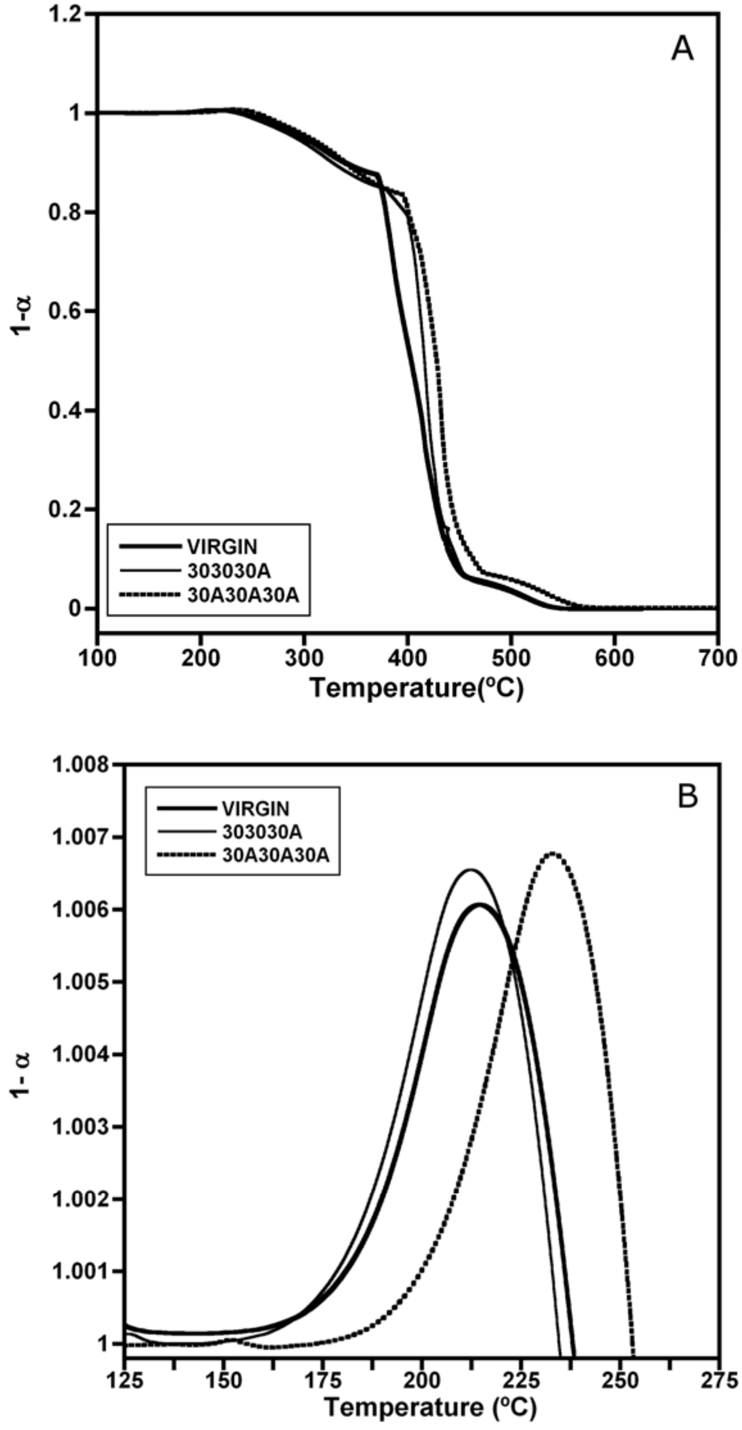
A
1-α
Temperature(°C)
VIRGIN
303030A
30A30A30A
B
1- α
Temperature (°C)
VIRGIN
303030A
30A30A30A

FIGURES 3A-E

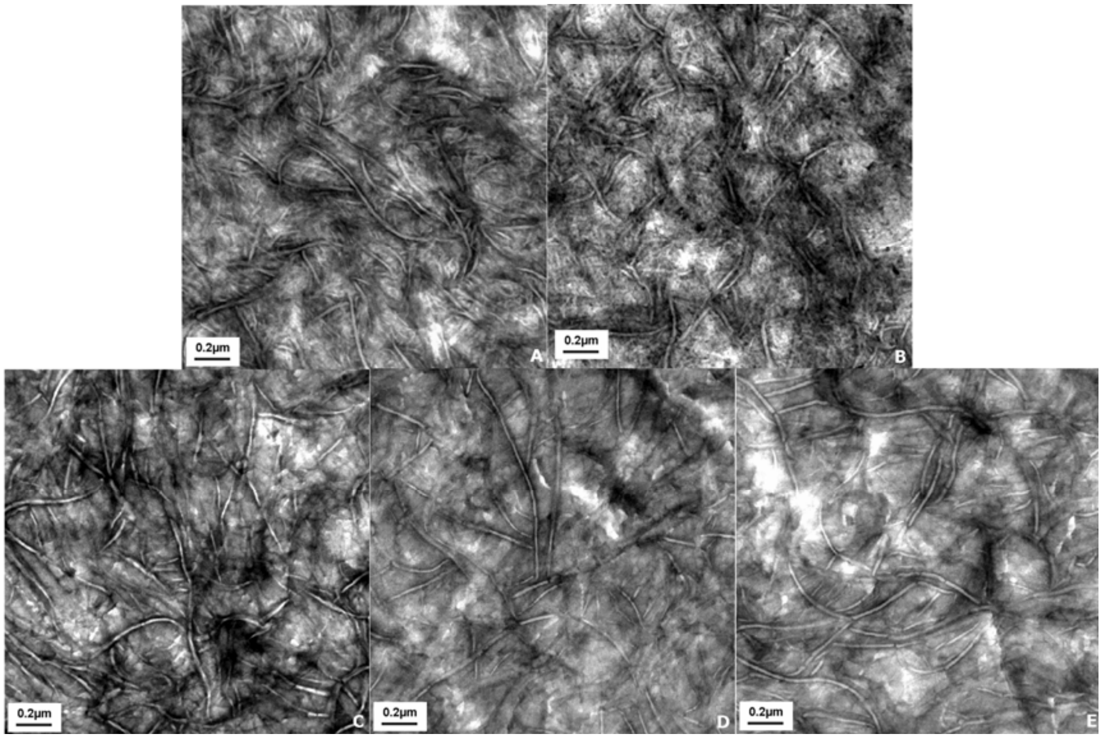

FIGURE 4

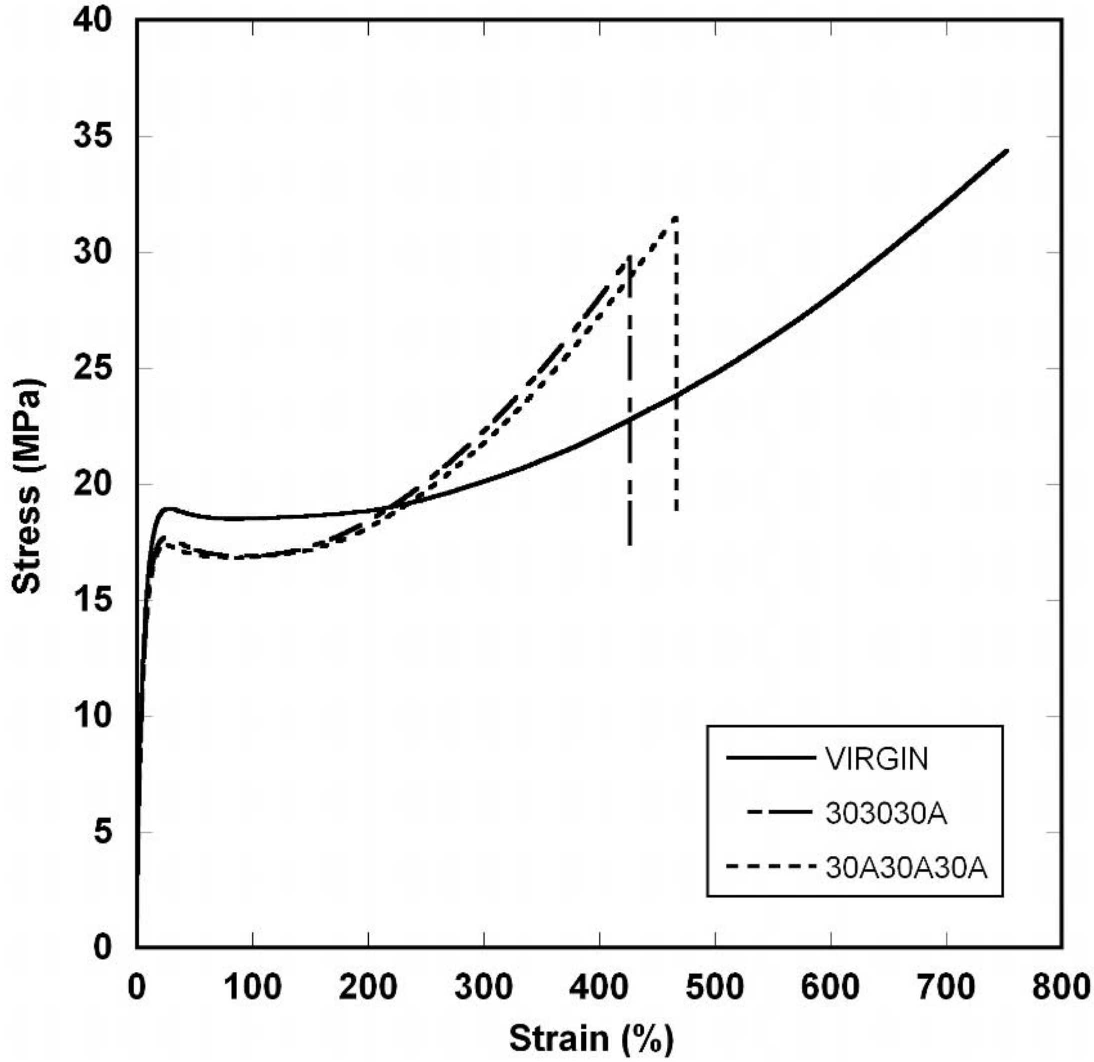
Stress (MPa)
Strain (%)
0
5
10
15
20
25
30
35
40
0
100
200
300
400
500
600
700
800
VIRGIN
303030A
30A30A30A

FIGURE 5

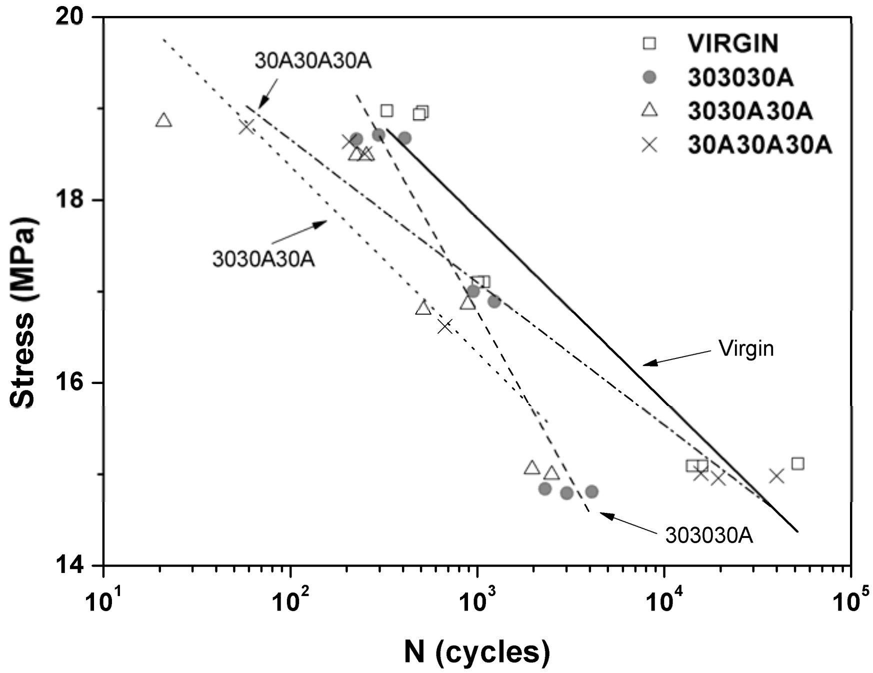
Stress (MPa)
N (cycles)
20
18
16
14
10^1
10^2
10^3
10^4
10^5
VIRGIN
303030A
3030A30A
30A30A30A
30A30A30A
3030A30A
Virgin
303030A

FIGURE 6

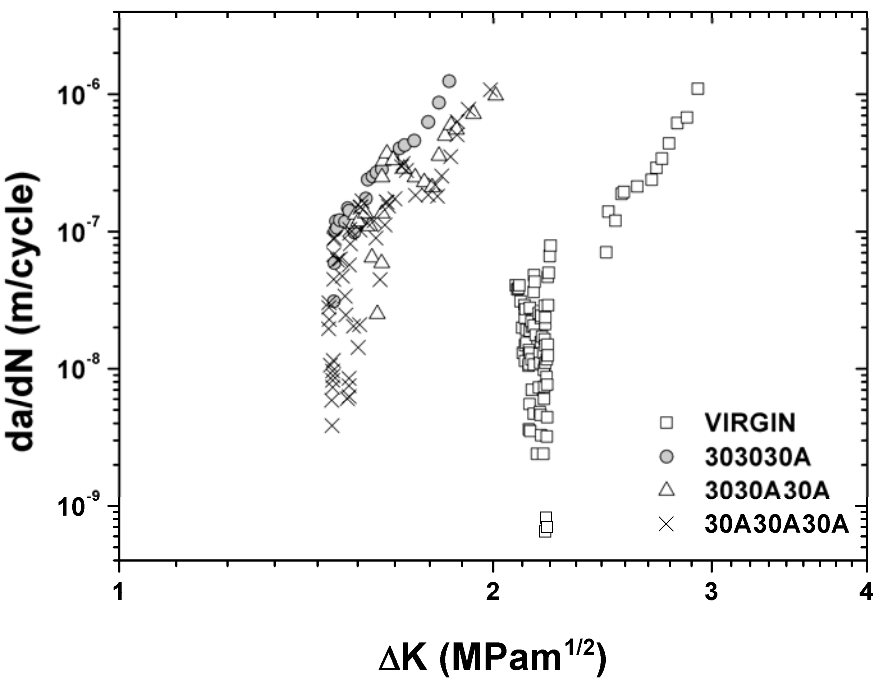
da/dN (m/cycle)
10^-6
10^-7
10^-8
10^-9
1
2
3
4
ΔK (MPam^1/2)
VIRGIN
303030A
3030A30A
30A30A30A

FIGURE 7

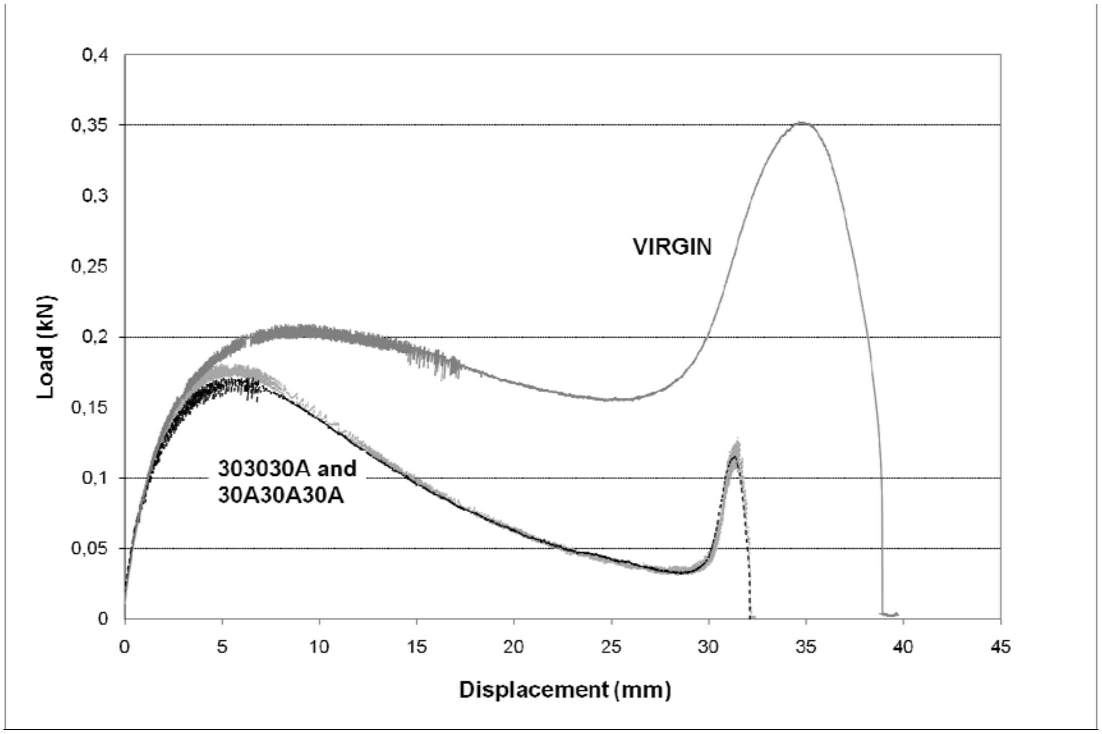
Load (kN)
0,4
0,35
0,3
0,25
0,2
0,15
0,1
0,05
0
VIRGIN
303030A and
30A30A30A
0
5
10
15
20
25
30
35
40
45
Displacement (mm)